Radiative and guided wave emission of Er^{3+} atoms located in planar multidielectric structures

H. Rigneault,[1,*] S. Robert,[1] C. Begon,[1] B. Jacquier,[2,†] and P. Moretti[2]
[1]*Laboratoire d'Optique des Surfaces et des Couches Minces, URA CNRS 1120, Ecole Nationale Supérieure de Physique de Marseille, Domaine Universitaire de St. Jérôme, 13397 Marseille Cedex 20, France*
[2]*LPCML, UMR CNRS 5620, Université Lyon 1, 43 Bd du 11 Nov. 1918, Villeurbanne, France*
(Received 10 June 1996)

Spontaneous emission of erbium atoms implanted in various planar multidielectric stacks is investigated. Computational and experimental analyses are performed so as to assess the amount of light leaking into the radiative and the guided modes of the structures. The key point is the demonstration of the dominant emission into the guided modes, even though the atoms are implanted in the spacer of a resonant microcavity structure. The result is of practical interest since it challenges the conventional idea about the electromagnetic confinement, which is likely to be reached within planar microcavities. [S1050-2947(97)07702-0]

PACS number(s): 42.50.Lc, 42.50.Ct, 42.55.−f, 42.60.−v

It is now common knowledge that the radiation pattern and the spontaneous emission rate of atomic sources depend on the structure of the vacuum-field modes surrounding the atom [1]. This structure can be modified by appropriate electromagnetic boundary conditions, and during the last decades this has been the subject of intense investigations [2]. Experimental demonstrations on atomic spontaneous emission control have been reported in the microwave [3] and in the infrared frequency range [4]. The optical domain has been investigated using dye molecules near a single mirror [5] or more recently in optical microcavities [6].

In this paper, we shall be primarily concerned with planar dielectric structures since it has been an open question for applications whether the cavity has to confine the waves in all three dimensions, or if a simpler planar structure can suffice. In the prior works, which have determined the radiation patterns of sources confined in planar microcavities, a lot of attention has been paid to the emission into the traveling-wave modes, which can escape the structures. These running modes called the full radiative modes (FRM) are of prime interest for applications, with a view to developing a highly directional emission normal to the structure's plane. Therefore, the radiation pattern in the infrared domain has been investigated and good agreement with the theoretical predictions has been published [7]. Furthermore, demonstration of a measurable change of spontaneous emission lifetime of Er^{3+} atoms due to cavity length variation in a Si-SiO_2 cavity has been reported [8] and confirmed by computation [9]. In this case, although leaky waveguide modes are included, only the emission into the FRM is concerned since the refractive index of the outer media is larger than or equal to that used to make the distributed Bragg reflectors (DBR). Nevertheless, because of the experimental difficulties associated with their detection, little attention has been paid to the emission into the discrete guided wave modes (GM) of planar structures, which exist when the refractive index of the outer media is lower than that used to make the DBR. These discrete GM exhibit evanescent waves in the air and in the substrate and are of prime interest when the substrate is made of glass [6]. In this case, complete knowledge of the amount of light relaxed into the GM is necessary to compute accurately that atomic lifetime. In this respect, recently, we have predicted theoretically that the spontaneous emission into these GM could be much stronger than that into the FRM [10]. The present paper reports an experimental confirmation of those predictions.

For this, we present a detailed investigation of the spontaneous emission properties of erbium atoms located in various planar dielectric structures coated on glass substrate. As mentioned before, our structures support discrete GM and, in that respect, differ from [8]. In particular, we provide a demonstration of the emission into the GM, and compare this power with the power emitted into the FRM of the structures. The results shed light on the striking limitation of the single-mode vacuum confinement expected for this type of planar microcavity, and are closely related to the inefficiency of those planar structures in inducing any significant lifetime modification, as reported previously [11].

Before reporting experimental results, let us describe the apparatus we have developed (Fig. 1). The spontaneous emission of the green transition ($\lambda_0=532$ nm) between the excited manifold $^4S_{3/2}$ and the ground manifold $^4I_{15/2}$ of Er^{3+} atoms implanted inside dielectric multilayers is investigated under the excitation provided by the $\lambda_p=488$ nm line of a cw Ar^+ laser. The pump beam is focused on the sample, exciting a 0.3-mm-diameter spot on the active side. A charge-coupled device (CCD) camera with a 50-mm focal length lens is connected to a personal computer, which performs a digital image processing, and displays the intensity relaxed by the Er atoms in every direction θ. Furthermore, a 550-nm cutoff filter (Shott OG) and a narrow-band interference filter centered on λ_0 are set between the samples and the camera to isolate the erbium photoluminescence signal. This first experimental configuration is designed to get the FRM radiation pattern from the air side. Let us specify that throughout this paper, the emission ''from the air side'' and ''from the substrate side'' will denote, respectively, the emission in the upper and lower outer media (see Fig. 1). In order to obtain the amount of light emitted into the GM, a decoupling prism ($SrTiO_3$) is placed against the sample 2 mm away from the

*FAX: (33) 04 91 28 80 67.
†FAX: (33) 04 72 43 11 30.

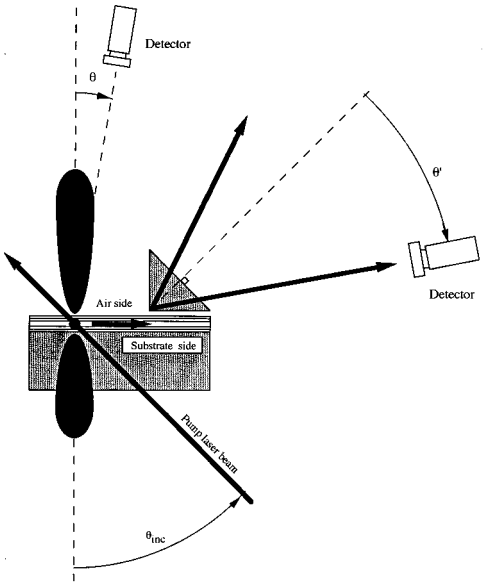

FIG. 1. Experimental apparatus.

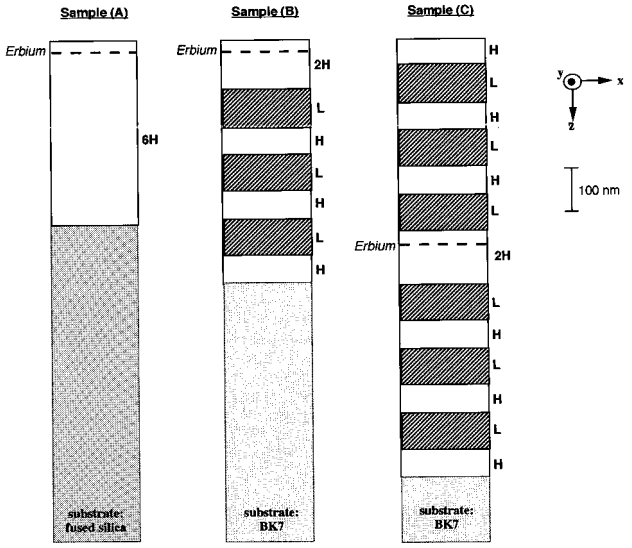

FIG. 2. Samples (A), (B), and (C).

excited atoms (see Fig. 1). The prism movements are controlled manually in the horizontal and vertical directions with an accuracy of 1 μm. This smart mechanical apparatus allows a precise control of the air gap between the sample and the prism, and performs a 100% decoupling efficiency [12]. Note that this important property has been tested experimentally in previous works using coupling and decoupling prisms [13]. The CCD camera can rotate around the prism's edge, giving for each angle θ' associated with a guided direction the amount of light that is relaxed into this particular GM. In addition, a polarizer is placed between the prism and the camera to separate transverse electric (TE) and transverse magnetic (TM) modes when they are decoupled at close angles.

All the layers considered here are made of tantalum pentoxyde (Ta_2O_5) and silicon dioxyde (SiO_2), respectively, for high (H) and low (L) refractive index materials. These materials are deposited on fused silica or on BK7 substrates by ion plating in a Balzers BAP 800 plant (deposition rate: 0.2 nm/s, plasma voltage: 70 V, plasma current: 52 A, pressure of O_2: 1.5×10^{-4} h Pa). Before coating, samples are cleaned by a standard four-step cleaning procedure.

Erbium implantation is performed in the Ta_2O_5 material using a DF4 Varian. Er ions are extracted from a Frieeman ion source fed with ErCl powder. The implantation fluence is 4.2×10^{15} ions/cm^2 and the energy is 300 keV. This leads to an Er peak concentration of 6.4×10^{20} ions/cm^3. Postimplantation thermal annealing is carried out on the samples at 400 °C during 1 h.

Figure 2 gives a schematic representation of the three samples considered in that work, and the position of the Er concentration peak (dashed line) is specified. Sample (A) is a tantalum pentoxide (Ta_2O_5) single layer whose optical thickness is $6\lambda_1/4$ ($\lambda_1=632.8$ nm, $n_H=2.23$). It is deposited on a fused silica substrate and the Er concentration peak lies 27 nm under the film-air interface. Sample (B) is a half-microcavity structure coated on BK7 glass. Its structure is $HLHLHL\ 2H$, where H and L stand, respectively, for a high and low refractive index layer whose optical thickness is $\lambda_0/4$ ($\lambda_0=532$ nm, $n_H=2.27$; $n_L=1.48$). Here again, the Er concentration peak is located 27 nm under the film-air interface. Sample (C) is a Fabry-Pérot-type microcavity structure coated on BK7 glass. Its structure is $HLHLHL\ 2H\ LHLHLH$ and its quality factor is given by $Q=\lambda_0/\Delta\lambda=40$. This sample has been manufactured in two steps; first a sample identical to sample (B) has been coated and implanted, secondly, another coating process has been performed.

The computation of the power emitted by an implanted microcavity into the FRM and the GM requires the determination of three key features of the microstructure: (1) the repartition profile of active erbium atoms in the stack; (2) the set of FRM; (3) the set of GM. We present first these computational steps for sample (A) in order to clarify this approach to the problem (see Fig. 3). Experimental results will be presented in parallel to illustrate the calculations.

The erbium profile in Ta_2O_5 is determined by using the ion implantation software PROFILECODE [14]. In Fig. 4(a) the roughly Gaussian-shaped repartition of erbium atoms is represented as a function of depth.

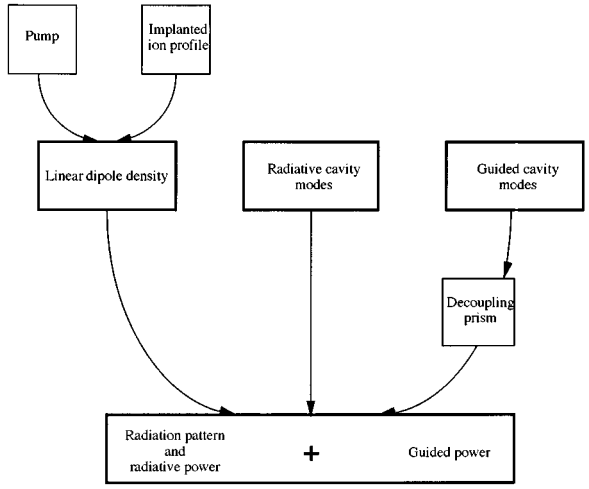

FIG. 3. Calculation chart.

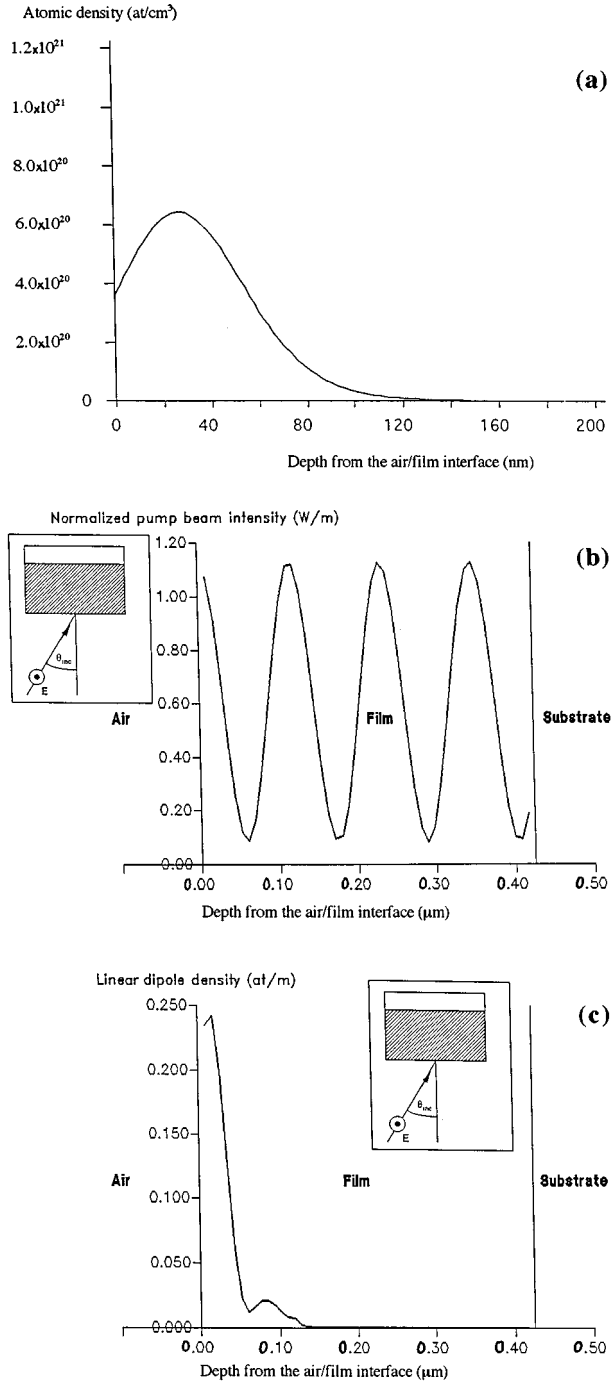

FIG. 4. (a) Erbium implantation profile. (b) Normalized pump beam intensity. (c) Linear dipole density. [Sample (A)—pump: $\theta_{inc}=55°$ incoming from the substrate side.]

As the pump field (TE polarization state, $\lambda_p=488$ nm) is modulated within the film, atoms are not equally excited. Pump field modulations are calculated assuming a plane wave of unit amplitude incoming on the air side or on the substrate side of the stack (depending on experimental conditions). Figure 4(b) exhibits the computed electric field profile obtained for a TE polarized pump beam incoming on sample (A) on the substrate side under an incident direction of $\theta_{inc}=55°$.

Thus, multiplying the Er profile of sample (A) [see Fig. 4(a)] by the pump field profile of Fig. 4(b), we can get the linear dipole density $\rho(z)$, which satisfies $\int_z \rho(z)dz=1$ [see

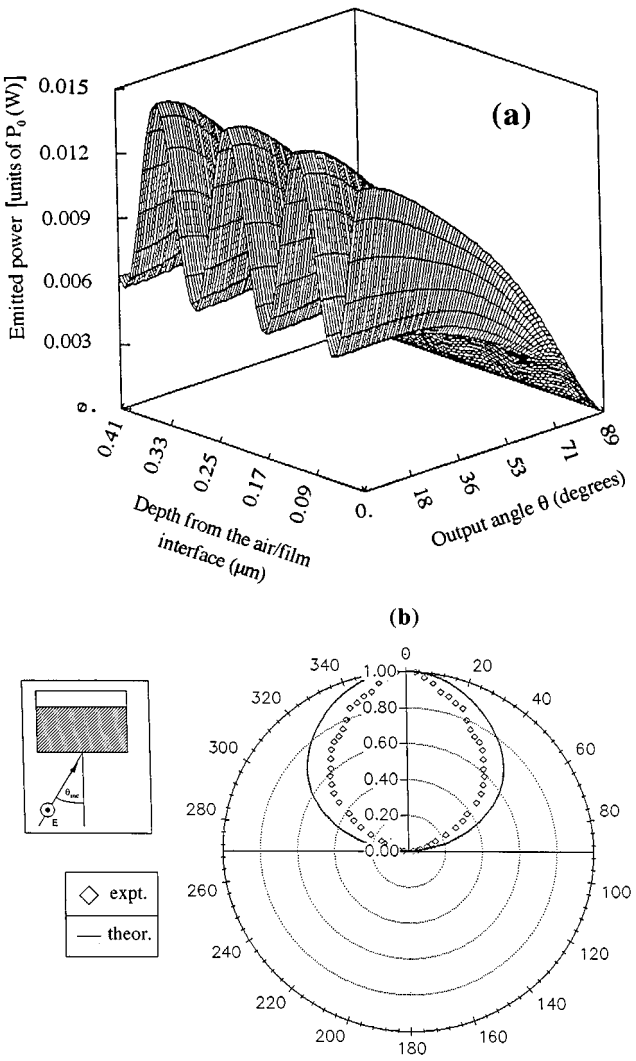

FIG. 5. (a) Normalized radiative emitted power as a function of atomic position and output angle. (b) Experimental and theoretical patterns. [Sample (A)—pump: $\theta_{inc}=55°$ incoming from the substrate side.]

Fig. 4(c)]. This linear dipole density acts as a single delocalized dipole, emitting the total power P_0 when located in the bulk material [10]. In the following calculations, this delo-

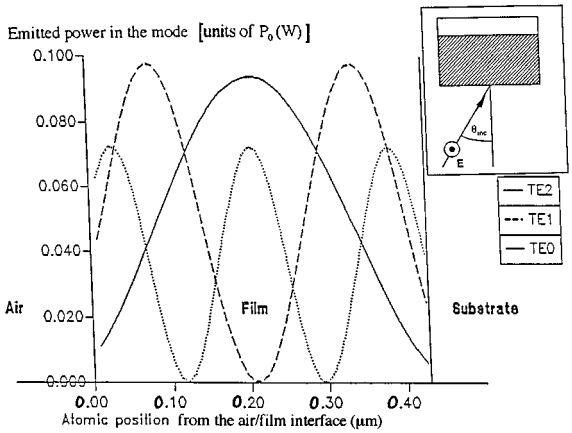

FIG. 6. Emitted power in TE modes as a function of atomic position. [Sample (A)—pump: $\theta_{inc}=23°$ incoming from the substrate side.]

TABLE I. Angular aperture at half-maximum intensity for theoretical and experimental radiation patterns.

	Theoretical values			Experimental values		
Sample	(*A*)	(*B*)	(*C*)	(*A*)	(*B*)	(*C*)
θ_{inc}°	55°	50°	50°	55°	50°	50°
P_{pump}	1 a.u.	1 a.u.	1 a.u.	294 mW	6 mW	2.5 mW
$\Delta\theta$°	65°	38°	14°	50°	36°	21°

calized dipole is considered as a three-dimensional dipole as is usually the case for erbium atoms located in amorphous host materials [15]. Note that if the incidence angle of the pump varies, so does the linear dipole density [16].

Then, as demonstrated in [10], spontaneous emission in planar multidielectric structures can be calculated using a complete set of orthogonal and normalized modes. It includes a continuous spectrum of radiation modes, which is composed of FRM and substrate modes, and a discrete spectrum of GM. Calculation and orthonormalization of those modes is performed for $\lambda_0=532$ nm corresponding to the Er green transition.

Let us consider first the power emitted into the FRM from the air side. Figure 5(a) shows the computed power emitted by a single dipole for every direction θ (in the range 0, 89°), and for every location of the dipole in the depth of sample (*A*). In this respect, it appears that at normal incidence ($\theta=0°$) four positions correspond to a maximum of emission ($0.015\ P_0$), and four contribute to a minimum ($0.006\ P_0$). Furthermore, for each atomic position the emitted power decreases with the increasing outgoing angle θ. Adding the various contributions of the linear dipole density $\rho(z)$, we can construct the radiation pattern in a plane perpendicular to the sample. Figure 5(b) presents the theoretical results (continuous line) and the experimental data (open square) recorded with our apparatus. Note quite good agreement between the curves: maximum of intensity in the normal direction, aperture angle at half maximum intensity (see Table I), and an extinction angle of approximately 70°.

New and more interesting results concern the power emitted by the atoms in the various GM. Sample (*A*) supports six guided modes (three for each polarization state). Figure 6 gives the computed emitted power in the various TE guided modes versus the dipole location in the stack. For example, an atom located 120 nm under the air-film interface emits roughly the same power in both TE0 and TE1 modes, while it has no significant contribution in the TE2 mode. More precisely, the amount of power emitted in each GM is obtained by multiplying the power curves given in Fig. 6 by the linear dipole density $\rho(z)$. In addition, the comparison with experimental data requires one to multiply the calculated powers by the angular transmittance of the prism-air interface corresponding to each GM direction.

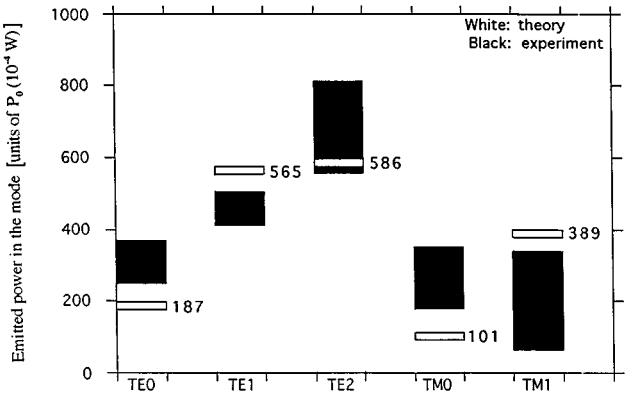

FIG. 7. Experimental and theoretical guided powers for TE0, TE1, TE2, TM0, and TM1 modes. [Sample (*A*)—pump: $\theta_{inc}=23°$ incoming from the substrate side.]

On the whole, Fig. 7 presents the theoretical (open bar) and experimental results (black bar) for sample (*A*) concerning the power emitted by the atoms in the various GM. Experimental data have been normalized in order to compare with calculations. The incident pump beam is incoming on the layer on the substrate side with an incident angle $\theta_{inc}=23°$. Note that the large black error bars represent the measurements we have performed for different positions of the laser spot on the sample. They reflect a relative inhomogeneity of the photoluminescence probably due to the ion implantation process. In spite of these experimental difficulties, orders of magnitude are in good agreement with the theory. Moreover, TE1 and TE2 guided powers are the strongest as expected in theory. Note that TM2 power is not reported on the graph because of mechanical limitations of the setup.

Additionally, in order to sharpen our investigation, we want to focus our attention on the ratio $R=P_{GM}/P_{FRM}$, where P_{FRM} and P_{GM} are, respectively, the powers emitted in the FRM and in the GM that are actually accessible with our experimental apparatus. Considering the power emitted in the five GM and the power emitted in the FRM from the air side, one finds $R_{exp}=38$ whereas computation gives $R_{th}=33$ ($\theta_{inc}=23°$; see Table II). This striking result shows that most of the power is relaxed into the GM in this simple single-layer structure. As the power emitted into the FRM is lower, we have increased the pump power to enhance the photoluminescence signal. As a result, we have exploited the linear dependence of the spontaneous emission power versus the pump power [17] to compare the GM and FRM measurements.

Similar investigations (GM and FRM radiation patterns,

TABLE II. Experimental and theoretical ratio $R=P_{GM}/P_{FRM}$, where P_{GM} and P_{FRM} are respectively the guided and radiative powers, which are experimentally accessible.

Sample	(*A*)	(*B*)	(*C*)
Theoretical ratio *R*	33	11	15
Experimental ratio *R*	38	7	16

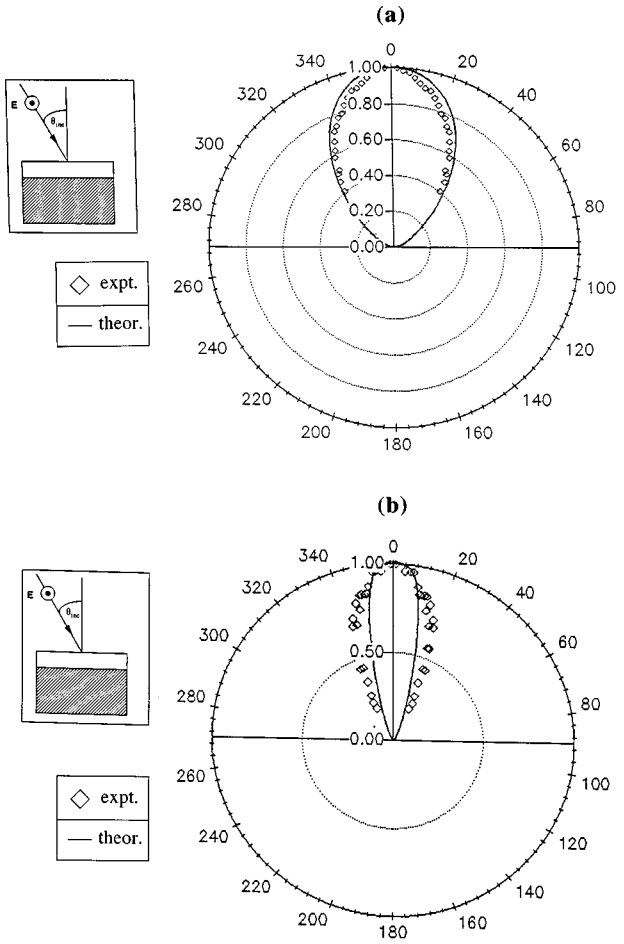

FIG. 8. (a) Sample (B): experimental and theoretical radiative patterns. (b) Sample (C): experimental and theoretical radiative patterns. [Pump: $\theta_{inc}=50°$ incoming from the air side.]

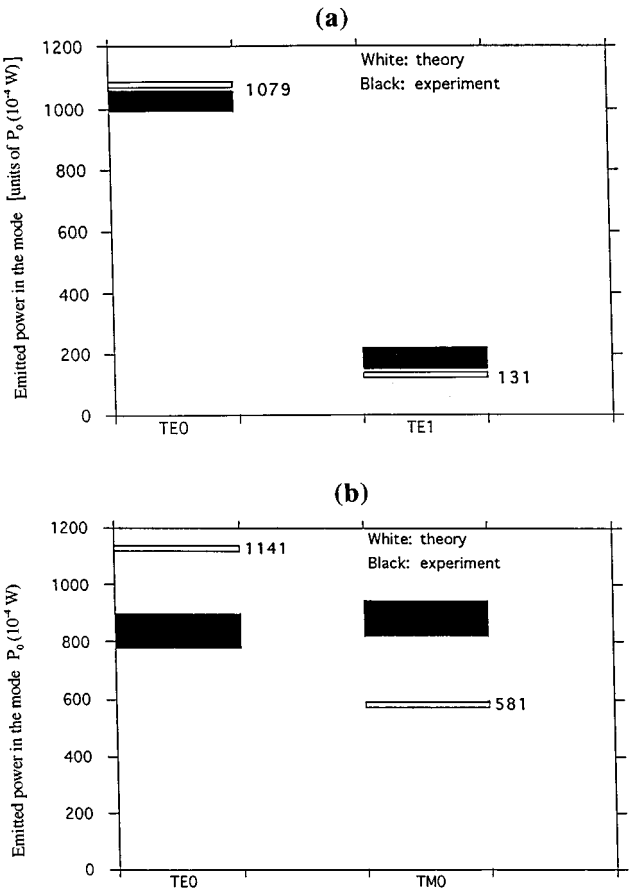

FIG. 9. (a) Sample (B): experimental and theoretical guided power for TE0 and TE1 modes: [Pump: $\theta_{inc}=29°$ incoming from the substrate side.] (b) Sample (C): experimental and theoretical guided power for TE0 and TM0 modes. [Pump: $\theta_{inc}=50°$ incoming from the substrate side.]

R ratio) are presented now for samples (B) and (C). We consider first the emission into the FRM from the air side. The theoretical (continuous line) and the measured (open square) diagrams for samples (B) and (C) are, respectively, represented on Figs. 8(a) and 8(b) when the pump beam is incoming on the air side of the samples with $\theta_{inc}=50°$. Experimental shapes are in good agreement with theory for both samples. The radiative emission of atoms located in sample (C) is more directive than in samples (A) and (B). Table I gives the theoretical and measured aperture angles $\Delta\theta$ corresponding to half-maximum intensity in the radiation patterns. Not reported on normalized Figs. 5(b), 8(a), and 8(b) is the intensity in normal direction, which appears to be about 100 times stronger for sample (C) than for sample (A) and 3 times stronger for sample (C) than for sample (B) (see the pump power in Table I). These results illustrate clearly the resonant effect of the microcavity. They confirm that photoluminescence is spatially affected by the cavity structure, in particular: the more pinched the radiation pattern is, the higher the emitted intensity in normal direction.

Consider now the GM. Samples (B) and (C) support, respectively, 5 and 9 GM. The emission into these various GM is predicted and detected to be dominant in the TE0 and TE1 modes for sample (B) and in the TE0 and TM0 modes for sample (C). This can be simply explained if we consider the overlapping integral between the atoms and the different GM field intensities. The good agreement between the measured and computed emitted powers in the GM is presented on Figs. 9(a) and 9(b). Table II gives the R ratio for the various samples considered. In all cases, the agreement between computations and experimental measurements is good, showing that most of the power is emitted into the guided modes of the structure.

In conclusion, we have investigated the spontaneous emission of erbium atoms located in various planar dielectric structures coated on a low refractive index glass substrate. Analysis has been performed for the FRM and we have provided the first evidence of the spontaneous emission in the GM, which are confined and propagate within the stack. Experimental results are in good agreement with theoretical calculations, and we have demonstrated that a large amount of light leaks into the guided modes of the structures. While postponing a detailed theoretical investigation of this process through the study of radiative lifetimes, these results point out a striking limitation in the single-mode confinement expected for this type of planar microcavities.

The authors thank Gérard Albrand for fabricating the coatings. The DRET (Direction des Recherches, Etudes et Techniques—French Ministry of Defense) and the CNRS (Centre National de la Recherche Scientifique) have sponsored this research.

[1] E. M. Purcell, Phys. Rev **69**, 681 (1946).

[2] D. Kleppner, Phys. Rev. Lett. **47**, 233 (1981); S. Haroche and D. Kleppner, Phys. Today **42** (1), 24 (1989); S. Haroche, in *Fundamental Systems in Quantum Optics* (North-Holland, Amsterdam, 1991), p. 767; H. Yokoyama, Science **256**, 66 (1992); Y. Yamamoto and R. E. Slusher, Phys. Today **46** (6), 66 (1993); H. O. Everitt, Opt. Photo. News, **3**, 18 (1992); P. R. Berman, *Cavity Quantum Electrodynamics* (Academic Press, New York, 1994).

[3] P. Goy, J. M. Raimond, M. Gross, and S. Haroche, Phys. Rev. Lett. **50**, 1903 (1983); D. Meschede, H. Walther, and G. Muller, Phys. Rev. Lett. **54**, 551 (1985); W. Jhe, A. Anderson, E. A. Hinds, D. Meschede, L. Moi, and S. Haroche, *ibid.* **58**, 666 (1987).

[4] G. Bjork, S. Machida, Y. Yamamoto, and K. Igeta, Phys. Rev. A **44**, 669 (1991); E. Snoeks, A. Lagendijk, and A. Polman, Phys. Rev. Lett. **74**, 2459 (1995).

[5] K. H. Drexhage, in *Progress in Optics*, edited by E. Wolf (North-Holland, Amsterdam, 1974), Vol. XII, p. 163.

[6] F. De Martini, G. Innocenti, G. R. Jacobovitz, and P. Mataloni, Phys. Rev. Lett. **59**, 2955 (1987); F. DeMartini, F. Cario, P. Mataloni, and F. Verzegnassi, Phys. Rev. A **46**, 4220 (1992).

[7] Y. Yamamoto, S. Machida, Y. Horikoshi, and K. Igeta, Optics Commun. **80**, 337 (1991).

[8] A. M. Vredenberg, N. E. J. Hunt, E. F. Schubert, D. C. Jacobson, J. M. Poate, and G. J. Zydzik, Phys. Rev. Lett. **71**, 517 (1993).

[9] C. C. Lin and D. G. Deppe, J. Appl. Phys. **75**, 4668 (1994); C. C. Lin, D. G. Deppe, and G. Lei, IEEE J. Quantum Electron. **30**, 2304 (1994).

[10] H. Rigneault and S. Monneret, Phys. Rev. A **54**, 2356 (1996).

[11] D. G. Deppe and C. Lei, J. Appl. Phys. **70**, 3443 (1991).

[12] It can be shown by a rigorous electromagnetic theory of the prism coupler that each guided mode at $\lambda_0=532$ nm is totally decoupled after 1 mm of propagation under the decoupling prism if one achieves an air gap thickness of the order of 100 nm. cf. H. Rigneault, F. Flory, and S. Monneret, Appl. Opt. **34**, 4358 (1995).

[13] F. Flory, H. Rigneault, N. Maythaveekulchai, and F. Zamkotsian, Appl. Opt. **32**, 5628 (1993).

[14] This software takes into account the Ta_2O_5 sputtering due to the heavy mass erbium ion penetration. The Er profile given by ProfileCode in Ta_2O_5 has been compared with secondary ion mass spectroscopy (SIMS) analysis and good agreement has been found. cf. H. Rigneault, F. Flory, S. Monneret, S. Robert, and L. Roux, Appl. Opt. **35**, 5005 (1996).

[15] N. J. Hunt, E. F. Chubert, D. L. Sivco, A. Y. Cho, R. F. Kopf, R. A. Logan, and G. J. Zydzik, in *Confined Electrons and Photons, New Physics and Application*, Vol. 340 of NATO ASI Series B, edited by C. Weisbuch and E. Burstein (Plenum, New York, 1995), p. 701.

[16] This can be related to the laser phase matching introduced by F. De Martini in the thresholdless microlaser experiment. cf. F. De Martini, M. Marocco, P. Mataloni, and D. Murra, J. Opt. Soc. Am. B **10**, 360 (1993).

[17] This linearity has been observed on every sample. cf. also B. A. Block and B. W. Wessels, Appl. Phys. Lett. **65**, 25 (1994).